

## Supplementary Material

### **Constructing a composite catalyst containing amorphous nickel hydroxide/crystalline lanthanum carbonate hydroxide for urea electrolysis**

Xing Gan<sup>1</sup>, Hua Jin<sup>1</sup>, Kun Xiong\*, Jianfeng Song, Shiqian She, Jia Chen, Haidong Zhang\*

Engineering Research Center for Waste Oil Recovery Technology and Equipment, Ministry of Education, College of Environment and Resources, Chongqing Technology and Business University, Chongqing 400067, China

\* Corresponding authors:

E-mail addresses: kunxiong@ctbu.edu.cn (K. Xiong); haidongzhang@ctbu.edu.cn (H. Zhang)

<sup>1</sup> These authors contributed equally to this work.

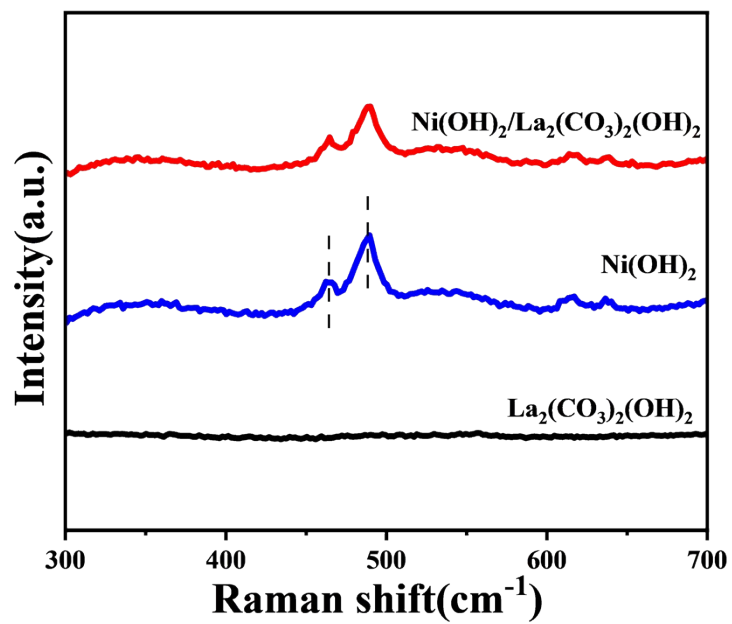


Fig. S1 Raman spectra of  $\text{Ni(OH)}_2/\text{La}_2(\text{CO}_3)_2(\text{OH})_2$ ,  $\text{Ni(OH)}_2$  and  $\text{La}_2(\text{CO}_3)_2(\text{OH})_2$ .

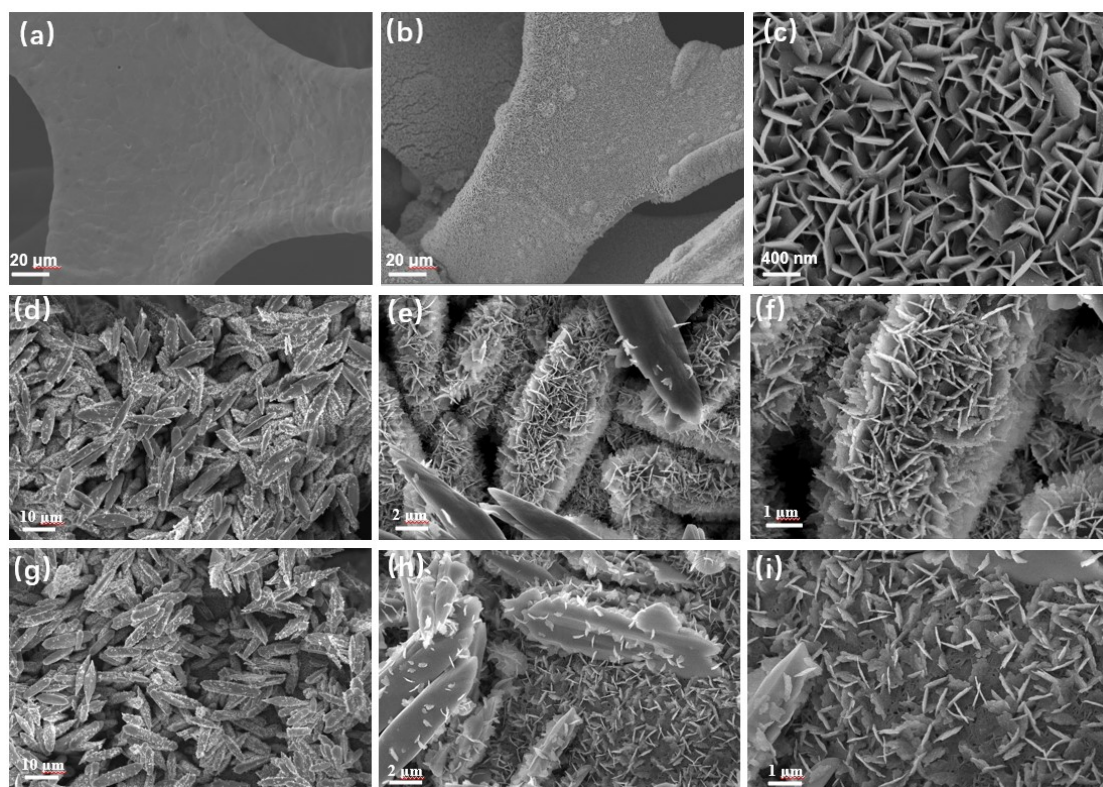


Fig. S2 FE-SEM images of catalysts at different magnifications : (a) NF, (b-c)  $\text{Ni(OH)}_2/\text{NF}$ , (d-f)  $\text{La}_2(\text{CO}_3)_2(\text{OH})_2/\text{NF}$  and (g-i)  $\text{Ni(OH)}_2/\text{La}_2(\text{CO}_3)_2(\text{OH})_2/\text{NF}$ .

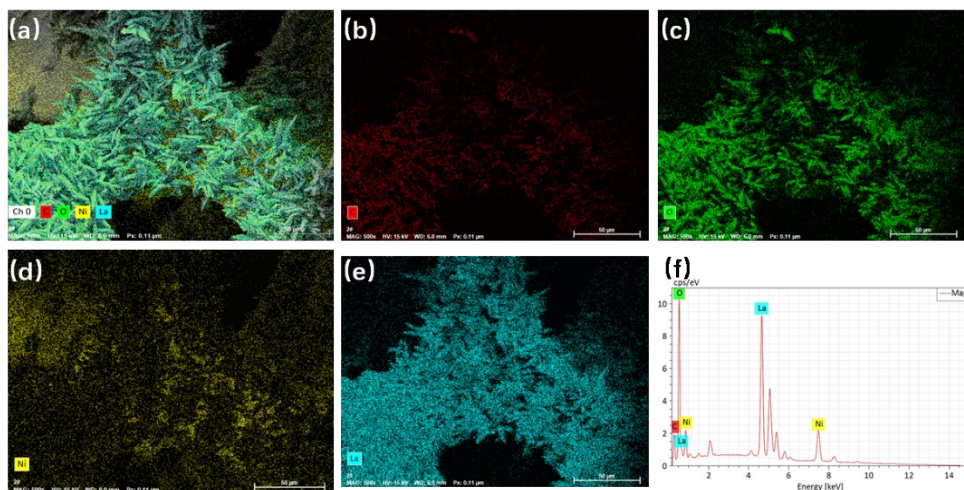


Fig. S3 EDS mapping images of the  $\text{Ni(OH)}_2/\text{La}_2(\text{CO}_3)_2(\text{OH})_2/\text{NF}$ .

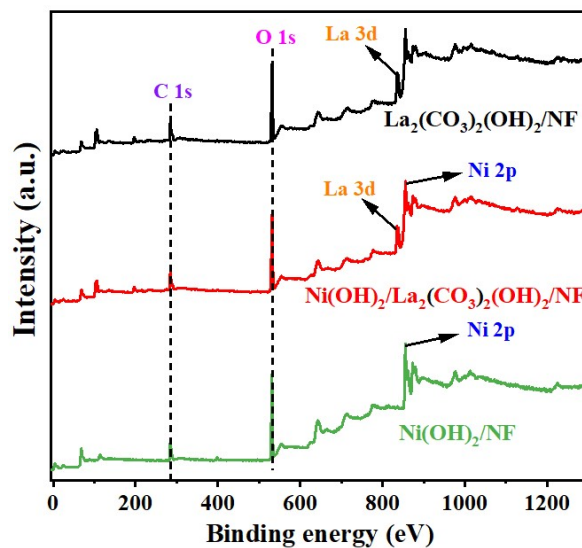


Fig. S4 XPS survey spectra of the  $\text{Ni(OH)}_2/\text{NF}$ ,  $\text{La}_2(\text{CO}_3)_2(\text{OH})_2/\text{NF}$ , and

$\text{Ni(OH)}_2/\text{La}_2(\text{CO}_3)_2(\text{OH})_2/\text{NF}$

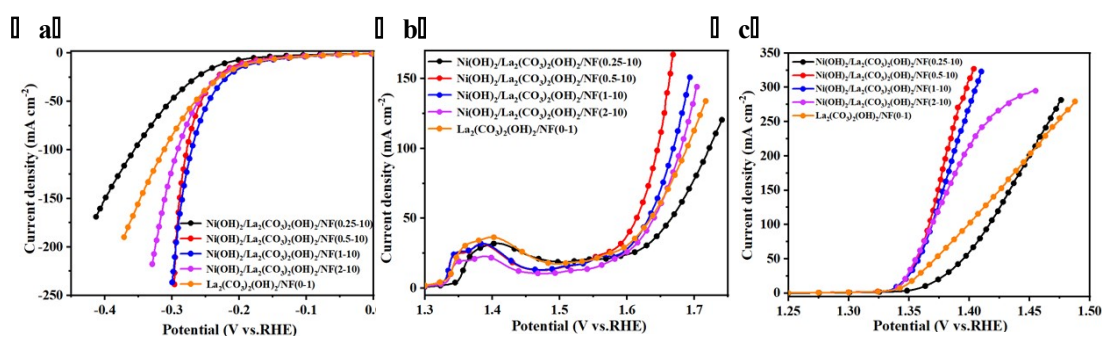
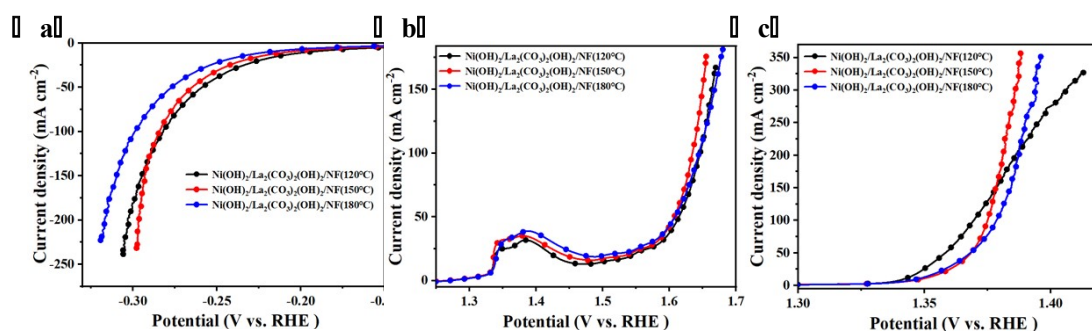
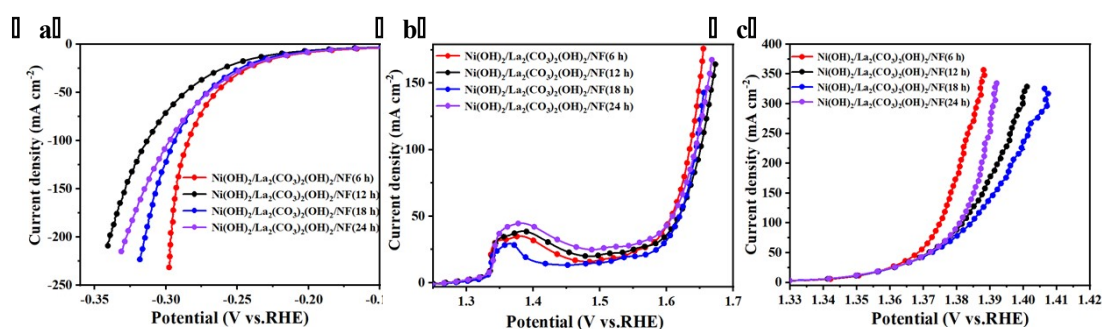


Fig. S5 LSV curves of the  $\text{Ni(OH)}_2/\text{La}_2(\text{CO}_3)_2(\text{OH})_2/\text{NF}$  under different Ni-to-La ratios: (a) HER,

(b) OER and (c) UOR.



**Fig. S6** LSV curves of the  $\text{Ni(OH)}_2/\text{La}_2(\text{CO}_3)_2(\text{OH})_2/\text{NF}$  under different hydrothermal temperatures: (a) HER, (b) OER and (c) UOR.



**Fig. S7** LSV curves of the  $\text{Ni(OH)}_2/\text{La}_2(\text{CO}_3)_2(\text{OH})_2/\text{NF}$  under different hydrothermal time: (a) HER, (b) OER and (c) UOR.

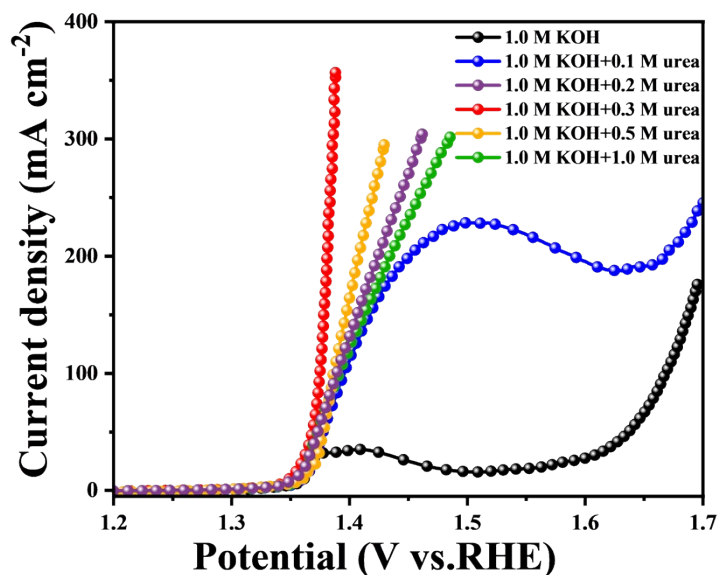


**Fig. S8** LSV curves measured for  $\text{Ni(OH)}_2/\text{La}_2(\text{CO}_3)_2(\text{OH})_2/\text{NF}$  in 1.0 M KOH with different concentrations ( $X=0.1, 0.2, 0.3, 0.5,$  and  $1.0$  M) of urea.

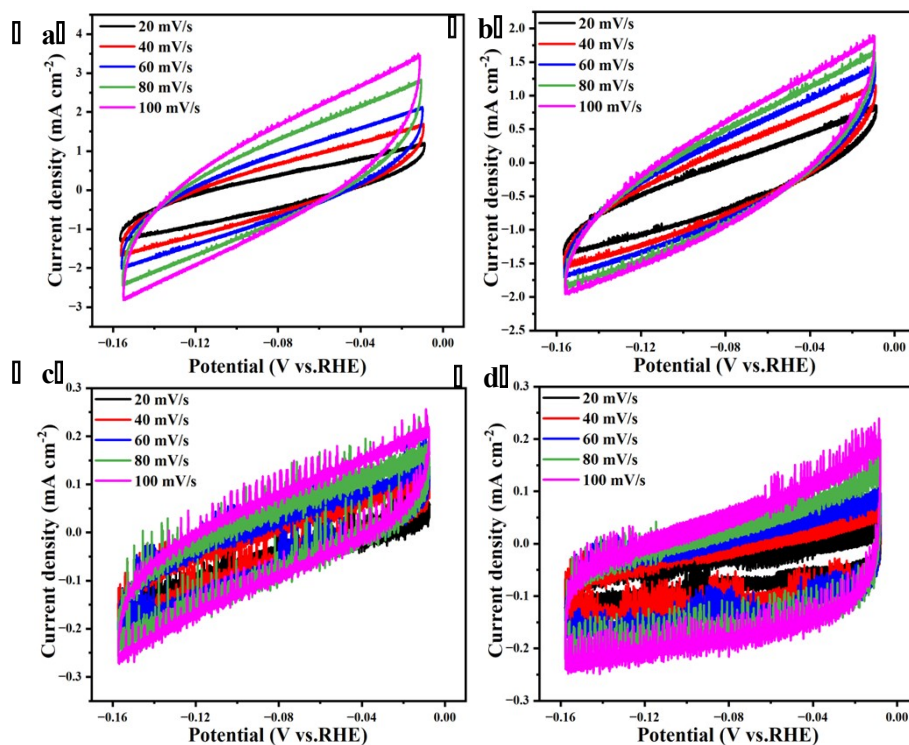


**Fig. S9** Cyclic voltammograms were taken in a potential range where no faradic processes were observed to measure the capacitive current from double layer charging. CV curves at different scan rate from  $20 \text{ mV s}^{-1}$  to  $100 \text{ mV s}^{-1}$ : (a)  $\text{Ni(OH)}_2/\text{La}_2(\text{CO}_3)_2(\text{OH})_2/\text{NF}$ , (b)  $\text{La}_2(\text{CO}_3)_2(\text{OH})_2/\text{NF}$ , (c)  $\text{Ni(OH)}_2/\text{NF}$ , and (d) NF.

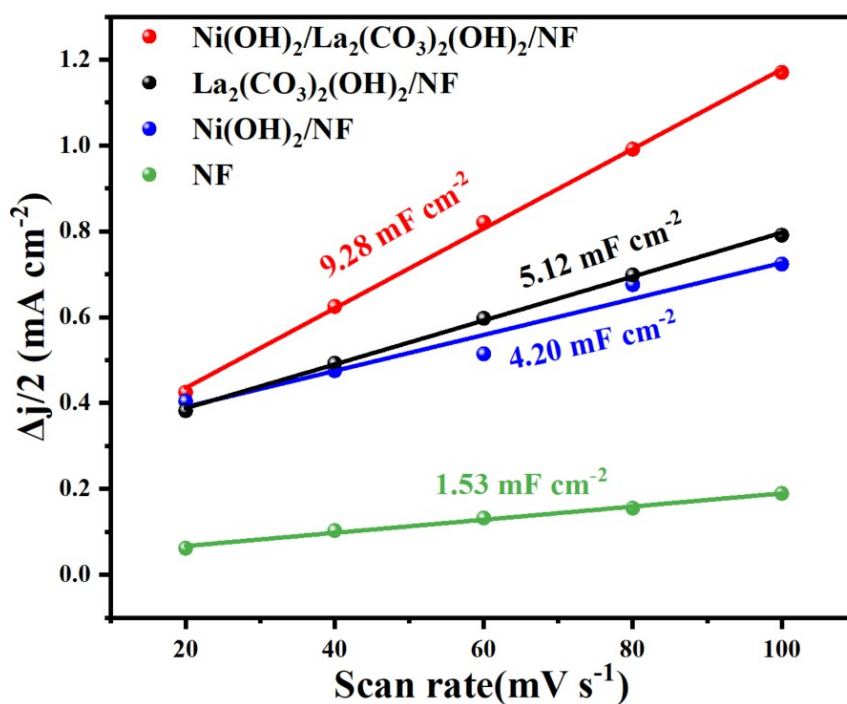


**Fig. S10** The HER performance of the as-prepared catalysts:  $C_{dl}$

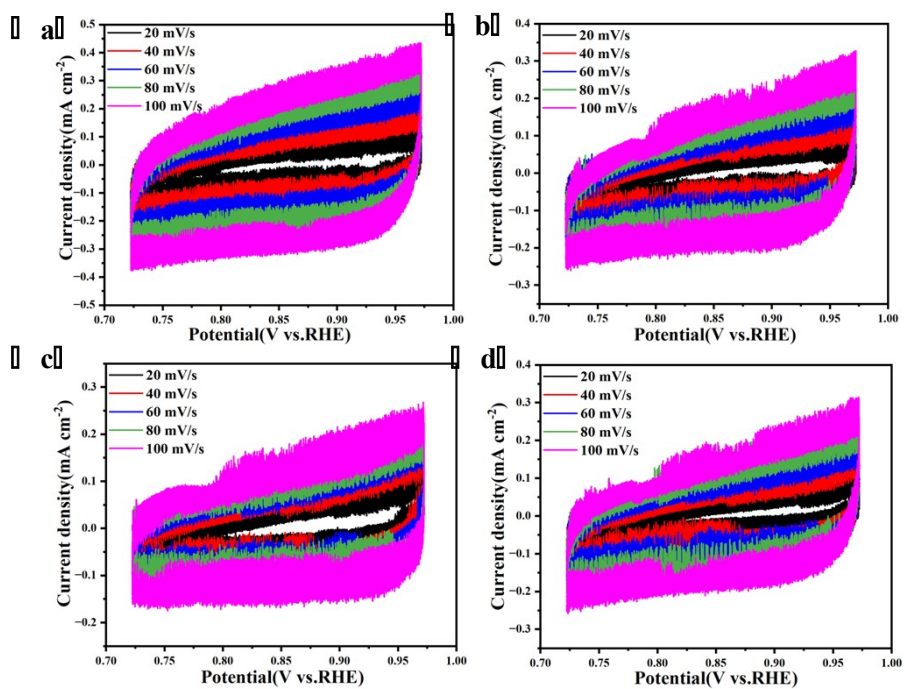


Fig. S11 CV curves at different scan rate from  $20 \text{ mV s}^{-1}$  to  $100 \text{ mV s}^{-1}$ : (a)

$\text{Ni(OH)}_2/\text{La}_2(\text{CO}_3)_2(\text{OH})_2/\text{NF}$ , (b)  $\text{La}_2(\text{CO}_3)_2(\text{OH})_2/\text{NF}$ , (c)  $\text{Ni(OH)}_2/\text{NF}$ , and (d) NF.

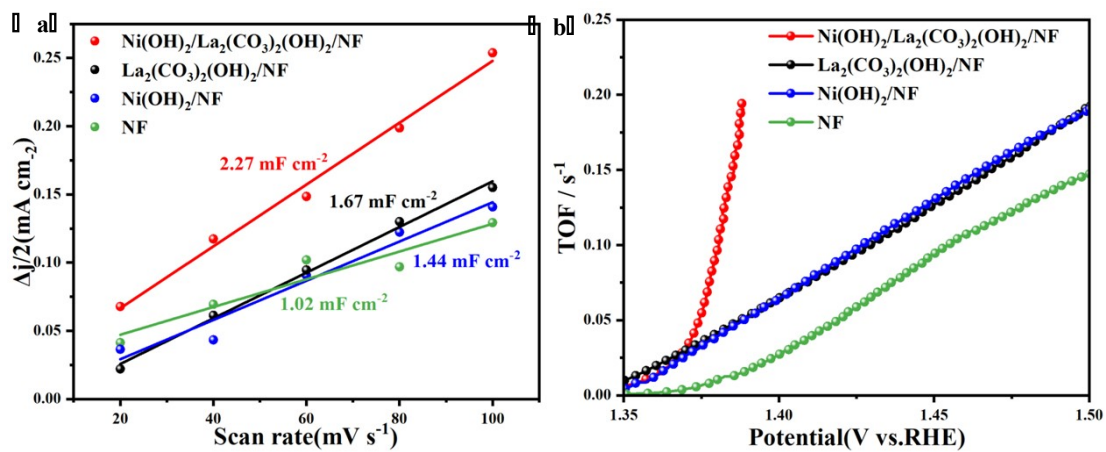


Fig. S12 The UOR performance of the as-prepared catalysts: (a)  $C_{dl}$ , (b) TOF curves.

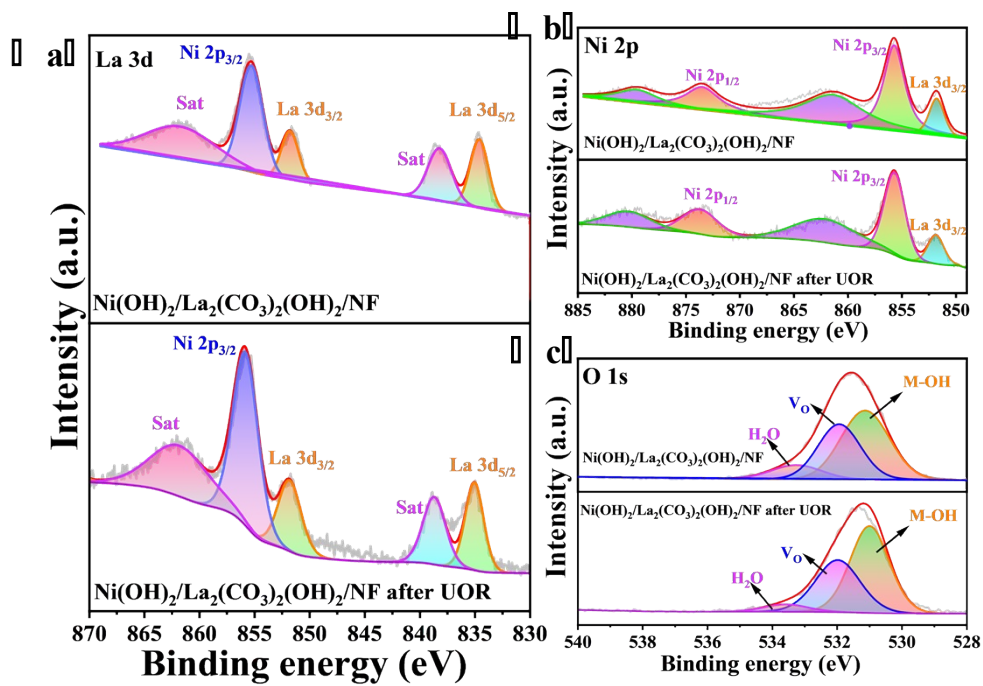


Fig. S13 Comparison of XPS spectra of  $\text{Ni(OH)}_2/\text{La}_2(\text{CO}_3)_2(\text{OH})_2/\text{NF}$  catalyst before and after

UOR stability testing.

**Table S1.** comparison of HER performance in alkaline electrolytes used for water splitting.

Electrolysts	Electrolyte	overpotential @10 mA cm <sup>-2</sup>	References
Ni(OH) <sub>2</sub> /La <sub>2</sub> (CO <sub>3</sub> ) <sub>2</sub> (OH) <sub>2</sub> /NF	1 M KOH	0.201 V	This work
Ni(OH) <sub>2</sub> /NF	1 M KOH	0.252 V	[4]
NiCo <sub>2</sub> S <sub>4</sub> /NF	1 M KOH	0.210	[5]
Ni <sub>2</sub> P/CNS	1 M KOH	0.315 V	[6]
Ni <sub>2</sub> P/Ni <sub>12</sub> P <sub>5</sub>	1 M KOH	0.234 V	[7]
Ni <sub>2</sub> P	1 M KOH	0.258 V	[7]
Ni <sub>12</sub> P <sub>5</sub>	1 M KOH	0.270 V	[8]
NiS <sub>2</sub> /NF	1 M KOH	0.255 V	[9]
NiS	1 M KOH	0.474 V	[10]
h-NiS	1 M KOH	0.205	[11]
Ni-CoCHH/NF	1 M KOH	0.248 V	[12]

**Table S2.** comparison of UOR performance in alkaline electrolytes used for water splitting.

Electrolysts	Electrolyte	Potential @10 mA cm <sup>-2</sup>	References
Ni(OH) <sub>2</sub> /La <sub>2</sub> (CO <sub>3</sub> ) <sub>2</sub> (OH) <sub>2</sub> /NF	1 M KOH + 0.3 M urea	1.348 V	This work
1% La:α-Ni(OH) <sub>2</sub>	1 M KOH + 0.33 M urea	1.567V	[13]
Ni/NiP	1 M KOH + 0.33 M urea	1.350V	[14]
Ni/NiS@CP	1 M KOH + 0.33 M urea	1.350V	[15]
Ce-Ni <sub>2</sub> P/NF	1 M KOH + 0.3 M urea	1.406V	[16]
NiFeMo	1 M KOH + 0.33 M urea	1.380V	[17]
Fc-NiCo-BDC	1 M KOH + 0.33 M urea	1.350	[18]
CoFe LDH/MOFs	1 M KOH + 0.33 M urea	1.450V	[19]
Ni-MOF-0.5	1 M KOH + 0.5 M urea	1.381V	[20]
Ni <sub>2</sub> P/Fe <sub>2</sub> P/NF	1 M KOH + 0.5 M urea	1.36V	[21]
N-NiO	1 M KOH + 0.5 M urea	1.390V	[22]

**Table S3.** comparison of overall urea splitting performance in alkaline electrolytes

Electrolysts	Electrolyte	Potential	References
Ni(OH) <sub>2</sub> /La <sub>2</sub> (CO <sub>3</sub> ) <sub>2</sub> (OH) <sub>2</sub> /NF	1 M KOH + 0.3 M urea	1.536 V@10 mA cm <sup>-2</sup>	This work
Ni(OH) <sub>2</sub> /La <sub>2</sub> (CO <sub>3</sub> ) <sub>2</sub> (OH) <sub>2</sub> /NF	1 M KOH + 0.3 M urea	1.689 V@100 mA cm <sup>-2</sup>	This work
CoS <sub>2</sub> -Ti	1 M KOH + 0.3 M urea	1.590 V@10 mA cm <sup>-2</sup>	[23]
Ni/C	1 M KOH + 0.3 M urea	1.600 V@10 mA cm <sup>-2</sup>	[24]
Co <sub>3</sub> O <sub>4</sub> /CC	1 M KOH + 0.3 M urea	1.710 V@10 mA cm <sup>-2</sup>	[25]
Ni@NCNT	1 M KOH + 0.5 M urea	1.560 V@10 mA cm <sup>-2</sup>	[26]
HC-NiMoS/Ti	1 M KOH + 0.5 M urea	1.590 V@10 mA cm <sup>-2</sup>	[27]
MnO <sub>2</sub> /MnCo <sub>2</sub> O <sub>4</sub> /Ni	1 M KOH + 0.5 M urea	1.550 V@10 mA cm <sup>-2</sup>	[28]
Ce-Ni <sub>2</sub> P/NF	1 M KOH + 0.3 M urea	1.780 V@100 mA cm <sup>-2</sup>	[16]
NiHCF/NF	1 M KOH + 0.33 M urea	1.800 V@100 mA cm <sup>-2</sup>	[29]
Ni <sub>0.85</sub> Se/CoSe <sub>2</sub> /NF	1 M KOH + 0.33 M urea	1.758 V@100 mA cm <sup>-2</sup>	[30]
CoP/MoO <sub>2</sub> /NF	1 M KOH + 0.5 M urea	1.690 V@100 mA cm <sup>-2</sup>	[31]

## References.

- [1] J. Ma, X. Wang, J. Song, Y. Tang, T. Sun, L. Liu, J. Wang, J. Wang and M. Yang, *Angew. Chem. Int. Ed.*, 2024, **63**, e202319153.
- [2] L. Zhu, Y.W. Cheng and Y.Q. Gong, *Fuel*, 2025, **397**, 135487.
- [3] J.Y. Chen, Y. Gao, W.W. Yang, Z.W. Li and K. Xiong, *Int. J. Hydrogen Energy*, 2024, **52**, 302-310.
- [4] Y.F. Cheng, Y.L. Li, Z.Y. Qiao, L.L. Hu, H.B. Geng, H.L. Dong, F. Liao and M.W. Shao, *J. Colloid Interface Sci.*, 2025, **679**, 600-608.
- [5] A. Sivanantham, P. Ganesan and S. Shanmugam, *Adv. Funct. Mater.*, 2016, **26**, 4661-4672.
- [6] Y. Li, P. Cai, S. Ci and Z.H. Wen, *ChemElectroChem*, 2017, **4**, 340-344.
- [7] S. Surendran, S. Shanmugapriya, S. Shanmugam, L. Vasylechko and R.K. Selvan, *ACS Appl. Energy Mater.*, 2018, **1**, 78-92.
- [8] P.W. Menezes, A. Indra, C. Das, C. Walter, C. Gobel, V. Gutkin, D. Schmei and M. Driess, *ACS Catal.*, 2017, **7**, 103-109.
- [9] J. Yu, G. Cheng and W. Luo, *J Mater Chem A*, 2017, **5**, 15838-15844.
- [10] N. Jiang, Q. Tang, M. Sheng, B. You, D.E. Jiang and Y.J. Sun, *Catal Sci Technol*, 2016, **6**, 1077-1084.
- [11] F. Yuan, S. Wang, G.X. Yang, J.H. Qin, M. Chen, T.T. Fan and J.T. Ma, *J. Colloid Interface Sci.*, 2023, **633**, 640-648.
- [12] W.T. Lu, X.W. Li, F. Wei, K. Cheng, W.H. Li, Y.H. Zhou, W.Q. Zheng, L. Pan and G. Zhang, *Electrochim. Acta*, 2019, **318**, 252-261.
- [13] Z. Wei, W. Sun, S. Liu, J.D. Qi, L.Y. Kang, J.C. Li, S.S. Lou, J.F. Xie, B. Tang and Y. Xie, *Particuology*, 2021, **57**, 104-111.
- [14] C.Q. Pei, Y.Y. Qian, S.Q. Chen, J. Hu, S.S. Wu, M.J. Zhou, B.A. Sun and T. Feng, *Sci. China Mater.*, 2025, **68**, 820-829.
- [15] S. A. Aladeemy, P. Arunachalam, M.S. Amer and A.M. Al-Mayouf, *Rsc Adv.*, 2025, **15**, 14-25.
- [16] K. Xiong, L.J. Yu, Y. Xiang, H.D. Zhang, J. Chen and Y. Gao, *J. Alloys Compd.*, 2022, **912**, 165234.
- [17] Z.H. Lv, Z.H. Li, X. Tan, Z.M. Li, R. Wang, M.J. Wen, X. Liu, G.X. Wang, G.W. Xie and L.H. Jiang, *Appl. Surf. Sci.*, 2021, **552**, 149514.
- [18] M. Li, H.C. Sun, J.M. Yang, M. Humayun, L.F. Li, X.F. Xu, X.Y. Xue, A.H. Yangjeh, K. Temst and C.D Wang, *Chem. Eng. J.*, 2022, **430**, 132733.
- [19] S. Huang, Y. Wu, J. Fu, P.J. Xin, Q. Zhang, Z.Q. Jin, J. Zhang, Z.J. Hu and Z.W. Chen, *Nanotechnology*, 2021, **32**, 385405.
- [20] S. Zheng, Y. Zheng, H. Xue and H. Pang, *Chem. Eng. J.*, 2020, **395**, 125166.
- [21] L. Yan, Y. Sun, E. Hu, J.Q. Ning, Y.J. Zhong, Z.Y. Zhang and Y. Hu, *J Colloid Interface Sci*, 2019, **541**, 279-286.
- [22] X.S. Xu, J. He, J.C. Li, J. Zhou, S.Q. Yu, T. Wang, C.L. Wu and Y. Wang, *Colloid Surface A*, 2024, **695**, 134112.
- [23] S. Wei, X. Wang, J. Wang, X.P. Sun, L. Cui, W.R. Yang, Y.W. Zheng and J.Q. Liu, *Electrochim. Acta*, 2017, **246**, 776-782.
- [24] L. Wang, L. Ren, X. Wang, X. Feng, J.W. Zhou and B. Wang, *ACS Appl. Mater. Interfaces*,

- 2018, **10**, 4750-4756.
- [25] S.D. Li, J.C. Fan, S.Y. Li, Y. Ma, J.H. Wu, H.G. Jin, Z.S. Chao, D. Pan, Z.H. Guo, J. Nanostruct. Chem., 2021, **11**, 735-749.
- [26] Q. Zhang, F. M. D. Kazim, S. Ma, K.G. Qu, M. Li, Y.G. Wang, H. Hu, W.W. Cai, Z.H. Yang, Appl. Catal. B- Environ., 2021, **280**, 119436.
- [27] X. Wang, J. Wang, X. Sun, S. Wei, L. Cui, W.R. Yang, J.Q. Liu, Nano Res., 2018, **11**, 988-996.
- [28] C. Xiao, S. Li, X. Zhang, D.R. MacFarlane, J. Mater. Chem. A, 2017, **5**, 7825-7832.
- [29] G. Kalaiyaran, D. Lee, J.W. Lee, M.J. Ko, ACS Appl. Mater. Interfaces, 2024, **16**, 69142-69152.
- [30] S.W. Yuan, Y.H. Wu, L. Huang, Z.J. Zhang, W.J. Chen, Y.X. Wang, J. Colloid Interface Sci., 2025, **683**, 981-994.
- [31] Z.W. Liu, Z.J. Lu, Y.L. Cao, J. Xie, J.D. Hu, A.Z. Hao, Inorg. Chem., 2024, **63**, 2803-2813.